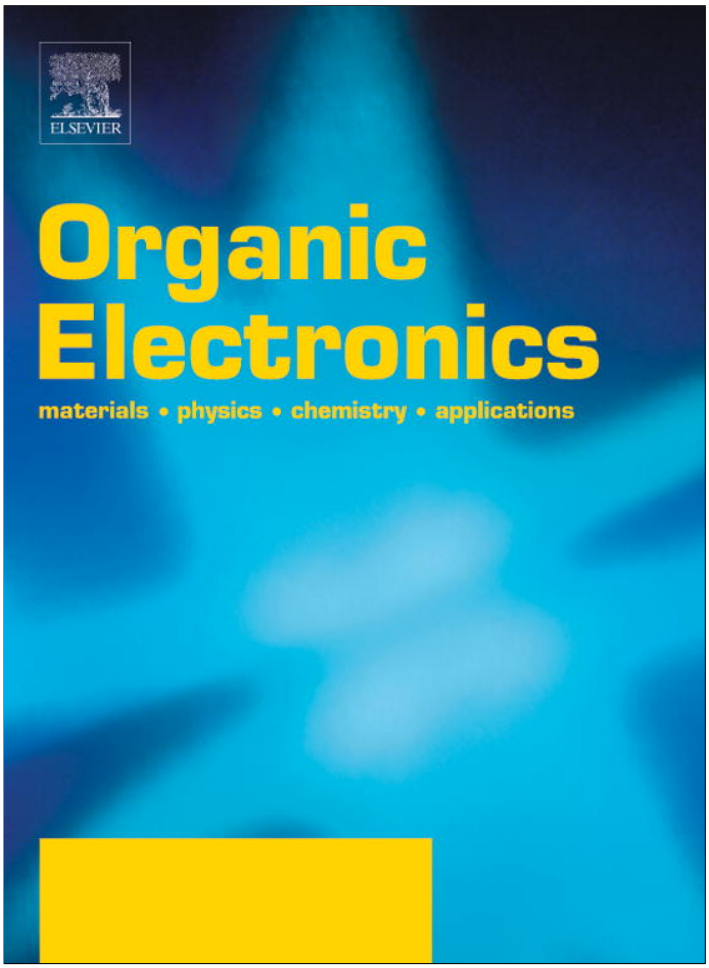

(This is a sample cover image for this issue. The actual cover is not yet available at this time.)

Organic Electronics 13 (2012) 3268–3275

Contents lists available at SciVerse ScienceDirect

Organic Electronics

journal homepage: www.elsevier.com/locate/orgel

An easily made thienoacene comprising seven fused rings for ambient-stable organic thin film transistors

Yagang Chen [a,b], Hao Chang [a,b], Hongkun Tian [a,*], Cheng Bao [a], Weili Li [a], Donghang Yan [a], Yanhou Geng [a,*], Fosong Wang [a]

[a] State Key Laboratory of Polymer Physics and Chemistry, Changchun Institute of Applied Chemistry, Chinese Academy of Sciences, Changchun 130022, PR China
[b] University of Chinese Academy of Sciences, Beijing 100049, PR China

ARTICLE INFO

Article history:
Received 27 August 2012
Received in revised form 20 September 2012
Accepted 23 September 2012
Available online 25 September 2012

Keywords:
Heteroacenes
Organic semiconductors
Organic thin-film transistors
Field-effect mobility

ABSTRACT

A novel easily made thienoacene-based organic semiconductor, i.e., dinaphtho[3,4-*d*:3′,4′-*d*′]benzo[1,2-*b*:4,5-*b*′]dithiophene (**Ph5T2**), was synthesized in high yield, and its thermal stability, electrochemical properties, thin-film morphology and field-effect mobility were investigated. **Ph5T2** exhibit excellent thermal stability with a decomposition temperature (T_d) of 427 °C. Thin-film X-ray diffraction (XRD) and atomic force microscopy (AFM) characterizations indicate that **Ph5T2** can form highly ordered films with large domain size on the *para*-sexiphenyl (6P)-modified substrates. Organic thin-film transistors (OTFTs) with top-contact geometry based on **Ph5T2** exhibit mobilities up to 1.2 $cm^2 V^{-1} s^{-1}$ in ambient. The devices are highly stable and exhibit almost no performance degradation during 3 months storage under ambient conditions with relative humidity up to 80%.

1. Introduction

High mobility and air stable organic semiconductors (OSCs) are of great current interest due to their application in organic thin film transistors (OTFTs) [1,2]. Acenes represent one of the most important classes of high mobility OSCs and a benchmark mobility of 5.0 $cm^2 V^{-1} s^{-1}$ has been demonstrated for pentacene-based OTFTs [3]. However, pentacene and larger acenes such as hexacene and heptacene have a drawback of poor air stability owing to their high-lying highest occupied molecular orbital (HOMO) energy levels [4–6].

Thienoacenes, which are obtained by replacing some or all phenyl rings in acenes with thiophene rings, have attracted more and more attention in past several years because of their low-lying HOMO energy levels and consequently good environmental stability [2]. A variety of thienoacene-type OSCs comprising 4–8 fused rings have been developed [7–27]. According to the chemical structures, these OSCs were divided into four classes by Takimiya: fused thiophenes, benzene-thiophene alternating molecules, acenedithiophenes, and diacene-fused thienothiophenes [2]. Several of them exhibited decent OTFT mobility beyond 1 $cm^2 V^{-1} s^{-1}$ [9,13,19,20–25]. For example, diacene-fused thienothiophenes with 4, 6 and 8 fused rings reported by Takimiya et al. all exhibited mobility >1 $cm^2 V^{-1} s^{-1}$ [20–25]. Müllen et al. reported a thienoacene with 5 rings which exhibited a mobility of 1.7 $cm^2 V^{-1} s^{-1}$ when dip-coating was employed for the fabrication of OTFTs [13]. Nevertheless, OSCs that combine several features, such as high mobility, good device stability and easy preparation which are required by future applications, are still scarce.

In the current paper, we reported a novel easily-made thienoacene-type semiconductor, i.e., dinaphtho[3,4-*d*:3′,4′-*d*′]benzo[1,2-*b*:4,5-*b*′]dithiophene (**Ph5T2**), comprising seven fused rings (Fig. 1). Different from diacene-fused thienothiophenes reported by Takimiya in which acene-terminals were β-position fused, it contains two α-position fused naphthyl terminals and a benzene-thiophene

* Corresponding authors.
E-mail addresses: hktian@ciac.jl.cn (H. Tian), yhgeng@ciac.jl.cn (Y. Geng).

1566-1199/$ - see front matter © 2012 Elsevier B.V. All rights reserved.
http://dx.doi.org/10.1016/j.orgel.2012.09.041

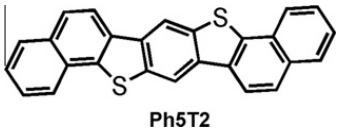

Ph5T2

Fig. 1. Chemical structure of thienoacene **Ph5T2**.

alternating central unit. OTFTs were fabricated by vacuum deposition, and a field-effect mobility of 1.2 $cm^2 V^{-1} s^{-1}$ along with a threshold voltage (V_T) of ~−10 V and a current on/off ratio (I_{on}/I_{off}) of >10^6 was achieved. Moreover, the device exhibited excellent ambient shelf-storage stability, and no obvious decay of mobility and I_{on}/I_{off} and shift of V_T were observed in a storage period of three months in ambient conditions with relative humidity up to 80%.

2. Experimental

2.1. Materials

All reactions were carried out under argon unless stated otherwise. Toluene was distilled over sodium and benzophenone. 2-(Naphthalene-6-yl)-1,3,2-dioxaborinane (**1**) [28] and 1,4-dibromo-2,5-bis (methylsulfinyl)benzene (**2**) [29,30] were synthesized according to literature procedures. Other reagents were obtained from commercial resources and used without further purification.

2.1.1. 1,4-Bis(naphthalene-6-yl)-2,5-bis(methylsulfinyl)benzene (*3*)

A mixture of **1** (2.57 g, 12.1 mmol), **2** (1.98 g, 5.5 mmol), $Pd(PPh_3)_4$ (127 mg, 0.11 mmol) and K_2CO_3 (6.68 g, 48.4 mmol) was degassed with argon, and then toluene (120 mL) and H_2O (24 mL) were added. The mixture was further purged with argon for 10 min and heated to 90 °C for 48 h, then poured into water for extraction with chloroform (3 × 80 mL). The combined organic layers were washed with brine, and dried over anhydrous $MgSO_4$. After the solvent had been removed, the residue was purified by column chromatography on silica gel with chloroform/ethyl acetate = 50:1 (v/v) as eluent to afford **3** as a white solid in a yield of 85% (4.67 g), ^{1}H NMR (600 MHz, $CDCl_3$): δ (ppm) 8.24 (s, 2 H), 8.01(s, 2 H), 7.99 (d, J = 8.4 Hz, 2 H), 7.90–7.95 (m, 4 H), 7.63 (dd, J = 1.8 Hz, J = 8.4 Hz, 2 H), 7.56–7.61 (m, 4 H), 2.40 (s, 6 H). ^{13}C NMR (150 MHz, $CDCl_3$): δ (ppm) 147.37, 139.73, 134.01, 133.24, 133.13, 128.98, 128.59, 128.34, 127.87, 127.13, 127.01, 126.43, 126.07, 41.60. Anal. Calcd for $C_{28}H_{22}O_2S_2$ (%): C, 73.98; H, 4.88. Found: C, 73.86; H, 4.52.

2.1.2. Dinaphtho[3,4-d:3′,4′-d′]benzo[1,2-b:4,5-b′]dithiophene (*Ph5T2*)

A 250 ml Schlenk flask was filled with **3** (2.30 g, 5.06 mmol), phosphorus pentoxide (210 mg) and trifluoromethanesulfonic acid (100 mL). The mixture was stirred for 72 h at room temperature and then poured into ice–water (100 mL). The yellow precipitate was collected by suction filtration and dried under vacuum. Demethylation was conducted in quinoline (100 mL) by heating at 180 °C for 24 h. When the suspension was cooled to room temperature, the precipitate was collected by filtration and washed successively with water and acetone, and then extracted with toluene in Soxhlet extractor. The crude product was purified by twice vacuum sublimation to afford **Ph5T2** as a white solid in a yield of 60% (1.18 g). ^{1}H NMR (400 MHz, $C_2D_2Cl_4$, 80 °C) δ (ppm) 8.76 (s, 2H), 8.26 (d, J = 7.2 Hz, 2H), 8.16 (d, J = 5.6 Hz, 2H), 8.00 (d, J = 6.0 Hz, 2H), 7.93 (d, J = 6.8 Hz, 2H), 7.65–7.59 (m, 4H). MALDI-TOF MS (reflection mode) m/z (%) 390.1 (100). Anal. Calcd for $C_{26}H_{14}S_2$ (%): C, 79.96; H, 3.61. Found: C, 79.93; H, 3.88.

2.2. Measurements

^{1}H and ^{13}C NMR spectra were recorded on a Bruker 600 MHz or 400 MHz spectrometer in $CDCl_3$ or $C_2D_2Cl_4$. Chemical shift was reported relative to an internal tetramethylsilane (TMS) standard for the measurements with $CDCl_3$ as solvent, while it was reported relative to the solvent signal for the measurements with $C_2D_2Cl_4$ as solvent. Elemental analysis was performed on a VarioEL elemental analysis system. Matrix-assisted laser desorption ionization time-of-flight (MALDI-TOF) mass spectra were recorded on a Bruker/AutoflexIII Smartbean MALDI mass spectrometer with dithranol as the matrix in reflection mode. TGA was carried out on a Perkin–Elmer TGA7 at a heating rate of 10 °C min^{-1} under nitrogen flow. UV–vis absorption was recorded on a Shimadzu UV-3600 UV–vis-NIR spectrometer. The bandgap was calculated accord-

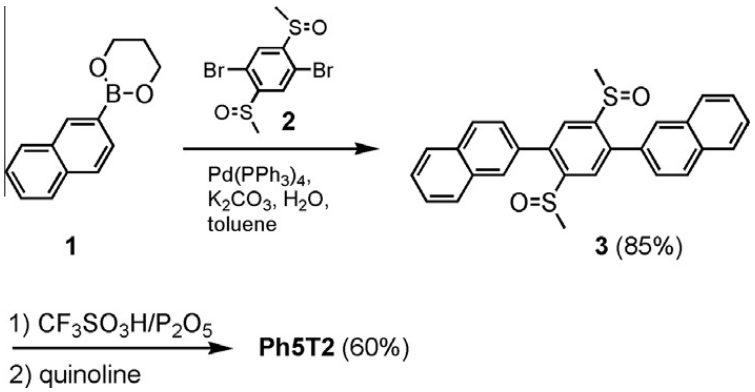

Scheme 1. Synthetic route of **Ph5T2**.

ing to the absorption onset of UV–vis spectra (E_g = 1240/λ_{onset} eV). Film cyclic voltammetry (CV) was performed on a CHI660a electrochemical analyzer with a three-electrode cell at a scan rate of 100 mV s^{-1}. Bu_4NPF_6 (0.1 mol L^{-1}) and anhydrous acetonitrile were used as electrolyte and solvent, respectively. A platinum plate (0.6 cm^2) with **Ph5T2** thin film prepared by vacuum deposition on it was used as the working electrode. A Pt wire and a saturated calomel electrode (SCE) were used as counter and reference electrodes, respectively. The potential was calibrated against the ferrocene/ferrocenium (Fc/Fc^+). The highest occupied molecular orbital (HOMO) level was estimated by the equation: $HOMO = -(4.80 + E_{ox}^{onset})\ eV$. Out-of-plane thin-film X-ray diffraction (XRD) was recorded on a Bruker D8 Discover thin-film diffractometer with Cu Kα radiation (λ = 1.541 Å). In-plane XRD of the thin film of **Ph5T2** were measured with a Rigaku SmartLab with a Cu *K*α source (λ = 1.541 Å) in air. Atomic force microscopy (AFM) measurements were performed in tapping mode on a SPA400HV instrument with a SPI 3800 controller (Seiko Instruments). Selected area electron diffraction (SAED) was performed on a JEOL JEM-1011 transmission electron microscope (TEM) operated at an acceleration voltage of 100 kV. In order to provide weaker-intensity beam and high contrast, dark field was used.

2.3. Fabrications and measurement of OTFTs

OTFTs were fabricated on heavily doped n-type Si wafers covered with 300 nm thick thermally grown SiO_2 (C_i = 10 nF cm^{-2}). The Si/SiO_2 substrates were carefully cleaned according to the literature procedure and then treated with octyltrichlorosilane (OTS), hexamethyldisilazane (HMDS) or octadecyltrichlorosilane (ODTS) to form a self-assembled monolayer (SAM) [31–33], then 40 nm **Ph5T2** film was deposited atop. Finally, Au drain and source electrodes (thickness 40 nm) were deposited in vacuum through a shadow mask. The channel length (L) and width (W) are 100 μm and 3000 μm, respectively. For OTFTs on 6P-modified substrates, 6P monolayer (2 nm) instead of OTS, HMDS or ODTS SAM was first deposited on the substrate [34], and other conditions are identical. The electrical measurements were performed with two Keithley 236 source/measure units at room temperature in ambient atmosphere. The mobility data were collected from more than 8 different devices. Like other organic semiconductors with HOMO energy levels lower than −5.5 eV [33–37], air-assistant mobility enhancement was observed in the course of measurement, and about one magnitude mobility enhancement was observed after ambient storage for 1–3 days. Therefore, all data reported in the paper are saturated values.

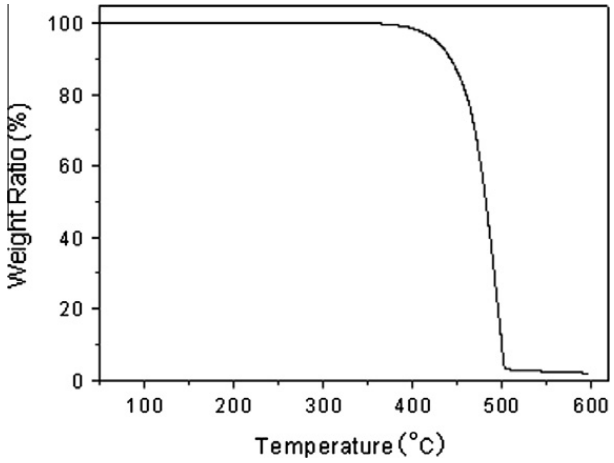

Fig. 2. TGA curve of **Ph5T2**.

3. Results and discussion

3.1. Synthesis and characterization

The synthesis of **Ph5T2** is depicted in Scheme 1. The synthetic route is relatively short and all reactions can be conducted in large scale. The starting materials (**1** and **2**)

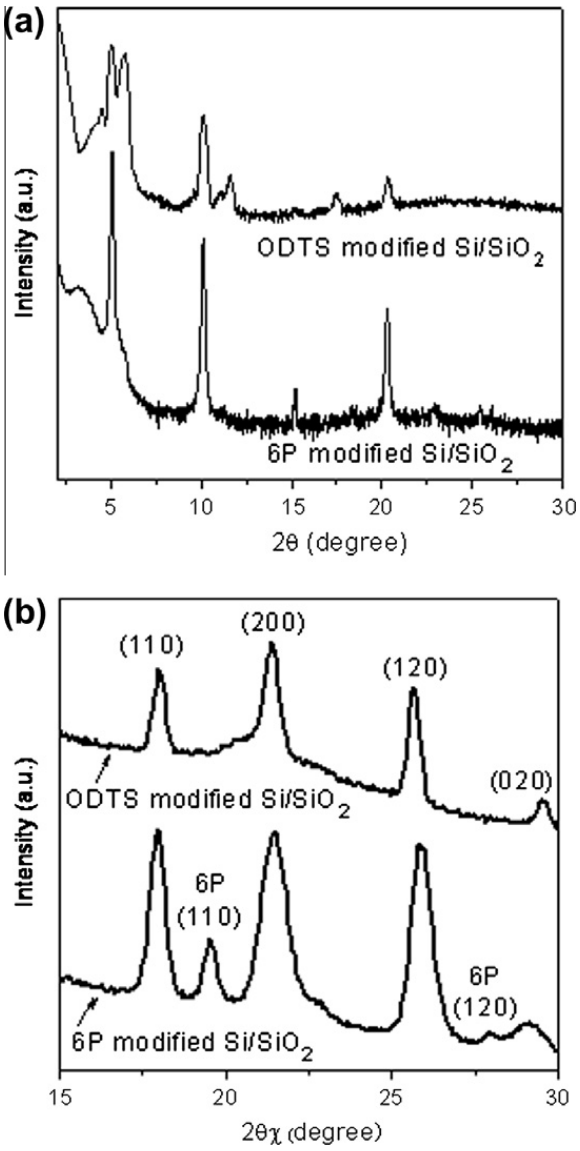

Fig. 3. Out-of-plane (a) and in-plane (b) XRD patterns of **Ph5T2** thin films deposited on the ODTS (top) and 6P (bottom) modified Si/SiO_2 substrates at T_{sub} = 80 °C.

were easily made from commercially available chemicals in large quantity [28–30]. The intermediate **3** was prepared by Suzuki coupling in a yield of 85%. The intramolecular ring-closing reaction was conducted by a modified reference procedure [10]. Subsequent purification by vacuum sublimation twice afforded **Ph5T2** as a white solid in a yield of 60%. The chemical structure was verified by high temperature ^{1}H NMR and MALDI-TOF mass spectra and element analysis (Figs. S1 and S2, Supporting Information). **Ph5T2** exhibited excellent thermal stability with a decomposition temperature (T_d) of 427 °C as measured by thermogravimetric analysis (TGA, Fig. 2).

3.2. Optical and electrochemical properties

The UV–vis spectrum of the vacuum-deposited thin film (~50 nm) revealed an absorption maximum at 396 nm. The optical band-gap is about 3.04 eV as estimated from the absorption edge (Fig. S3, Supporting Information), which is similar to that of dinaphtho[2,3-*b*:2′,3′-*f*]thieno[3,2-*b*]thiophene (**DNTT**) (3.0 eV) [21] but much larger than that of heptacene (1.5 eV) [6]. Thin-film cyclic voltammograms (CV) of **Ph5T2** were measured to estimate its energy levels. The HOMO level of **Ph5T2** was determined to be −5.85 eV (Fig. S4, Supporting Information). The low HOMO level implies that **Ph5T2** should be an environment-stable organic semiconductor. However, the HOMO level of **Ph5T2** is much lower than the work function of Au, which may result in a high hole injection barrier at the interface between Au and **Ph5T2** films in OTFT devices.

3.3. Thin film morphology

Microstructures of the films of **Ph5T2** on Si/SiO_2 substrates modified with different surface treatment reagents were studied by thin film XRD. The films on ODTS, HMDS or OTS SAM modified substrates exhibited similar XRD patterns. Fig. 3a shows the out-of-plane XRD pattern of **Ph5T2** film deposited on ODTS modified substrate at a substrate temperature (T_{sub}) of 80 °C. Clearly, two kinds of molecular arrangement modes were coexistent. The diffraction peaks, which are relative to the molecular length, can be divided into two groups with *d*-spacings of 17.45, 8.73, 5.82 and 4.36 Å and 15.17, 7.60 and 5.05 Å, respectively. This suggests that **Ph5T2** molecules stand on the substrate with different title angles. Since the molecular length is 18.05 Å as estimated from MM2 calculation, some molecules are nearly perpendicular to the substrate and the others lay on the substrate with a title angle of ~33°. Meanwhile, polymorphism of **Ph5T2** was observed in the powder XRD (Fig. S5, Supporting Information). This polymorphism has also been reported for benzo[1,2-*b*:4,5-*b*′]bis[*b*]benzothiophene (**BBBT**) [2], whose vacuum processed OTFTs exhibited a mobility as low as 2.4×10^{-3} $cm^2 V^{-1} s^{-1}$. The in-plane packing structure of **Ph5T2** film was also studied. As shown in Fig. 3b, four strong diffraction peaks at 18.0°, 21.4°, 25.6° and 29.5° were observed, corresponding to *d*-spacings of 4.92, 4.14, 3.47 and 3.02 Å, respectively, indicating that the thin-film are in-plane highly ordered.

We have reported that the continuous and highly ordered films with larger grain sizes of some OSCs could be prepared by depositing the materials on *para*-sexiphenyl (*p*-6P) monolayer modified Si/SiO_2 substrates, leading to the remarkable improvement in device performance [34,38,39]. Therefore, we also fabricated **Ph5T2** films on 6P-modified substrates. Induced by 6P layer, highly ordered thin films with only one crystalline phase in which the molecules were nearly perpendicular to the substrate were obtained. From SAED patterns, the in-plane lattice parameters $d_{(200)}$ and $d_{(010)}$($d_{(200)}$ = 4.20 Å, $d_{(010)}$ = 6.00 Å, γ = 90°) of **Ph5T2** are much larger than those of 6P ($d_{(200)}$ = 3.92 Å, $d_{(010)}$ = 5.59 Å, γ = 90°), as shown in Fig. S6 (Supporting Information). Meanwhile, the a^* and b^* axis of **Ph5T2** are parallel to the a^* and b^* axis of 6P, respec-

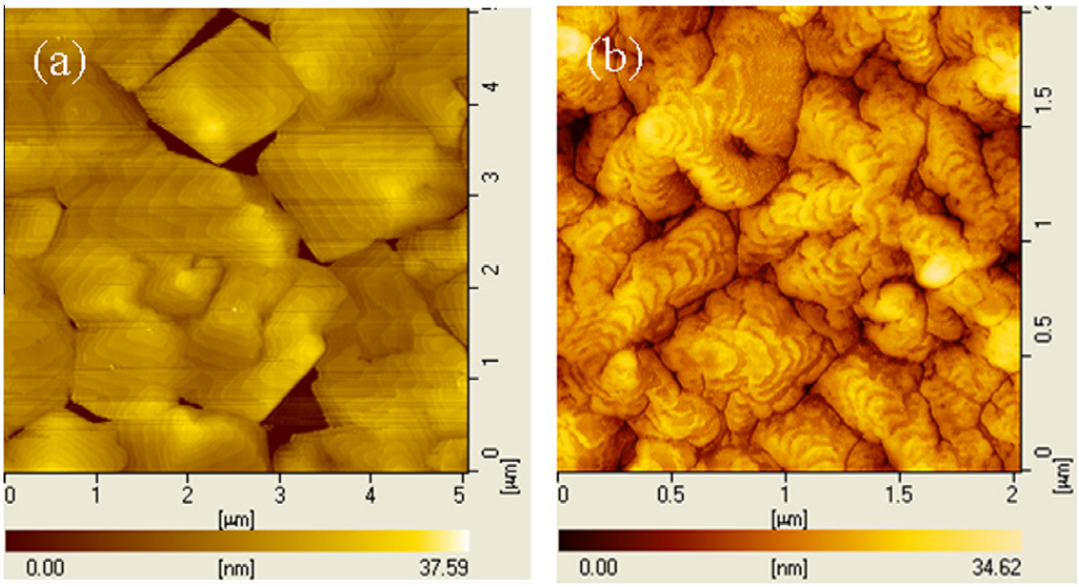

Fig. 4. AFM images of **Ph5T2** thin films on ODTS (a) and 6P (b) modified Si/SiO_2 substrates at T_{sub} = 80 °C.

tively. This indicates an incommensurate epitaxy growth of **Ph5T2** on 6P layer. As shown in Fig. 3a, the out-of-plane XRD pattern exhibited strong and sharp diffraction peaks up to four orders with the primary peak at 5.06° (*d*-spacing of 17.45 Å). In the in-plane XRD pattern (Fig. 3b), four strong diffraction peaks at 18.0°, 21.5°, 25.9° and 29.5° were observed, corresponding to *d*-spacings of 4.92, 4.13, 3.44 and 3.02 Å, respectively. **Ph5T2** molecules adopted the herringbone packing in the film as indicated by the SAED pattern, and therefore we can assign these peaks as (110), (200), (120) and (020). The similar in-plane XRD pattern were also found for diacene-fused thienothiophenes with 4, 6 and 8 fused rings reported by Takimiya et al. [22,25,40], Since the large HOMO coefficients on the sulfur atoms from the calculated frontier orbital (DFT B3LYP/6–31 g) (Fig. S7, Supporting Information) were also observed for **Ph5T2**, this packing structure should endow **Ph5T2** films two-dimensional (2D) carrier transport behavior like previous report on diacene-fused thienothiophenes by Takimiya et al. [2].

Fig. 4 depicts the atomic force microscopic (AFM) images of **Ph5T2** thin-films deposited on ODTS and 6P-modified substrates. On the ODTS-modified substrate, **Ph5T2** exhibited a layer-by-layer growth characteristic. However, poor connection between the crystalline domains was observed, probably due to the coexistence of two phases as revealed by the thin-film XRD pattern, which is detrimental to the charge carrier transport. In contrast, **Ph5T2** film deposited on the 6P-modified substrate exhibited dendrite crystalline morphology with tighter interconnection between crystalline grains. This type of morphology was also found for the film of pentacene [41]. Above morphology difference indicates that the surface properties of substrate have an important effect on the arrangement of **Ph5T2** molecules.

Table 1
OTFT device performance of **Ph5T2** on ODTS- or 6P-modified Si/SiO_2 substrates.

Surface–treatment reagent	T_{sub} (°C)	μ_{max} (μ_{ave}) ($cm^2\ V^{-1}\ s^{-1}$)	V_T (V)	I_{on}/I_{off}
ODTS	60	0.34 (0.26)	−16 to −26	10^6
	80	0.36 (0.29)	−14 to −25	10^6
	100	0.079 (0.057)	−24 to −29	10^5
6P	60	0.95 (0.83)	−15 to −22	10^6
	80	1.2 (1.0)	−10 to −18	10^6
	100	0.88 (0.73)	−13 to −22	10^6

3.4. Properties of OTFTs

OTFTs were fabricated with a bottom-gate and top-contact configuration. The Si/SiO_2 substrates were first modified with ODTS SAM or 6P monolayer. **Ph5T2** (40 nm) was then vacuum-deposited on the top at different T_{sub}. Finally, gold source and drain electrodes (40 nm) were evaporated through a shadow mask with a channel width (W) of 3000 μm and a channel length (L) of 100 μm, respectively. Table 1 summarizes the OTFT performance

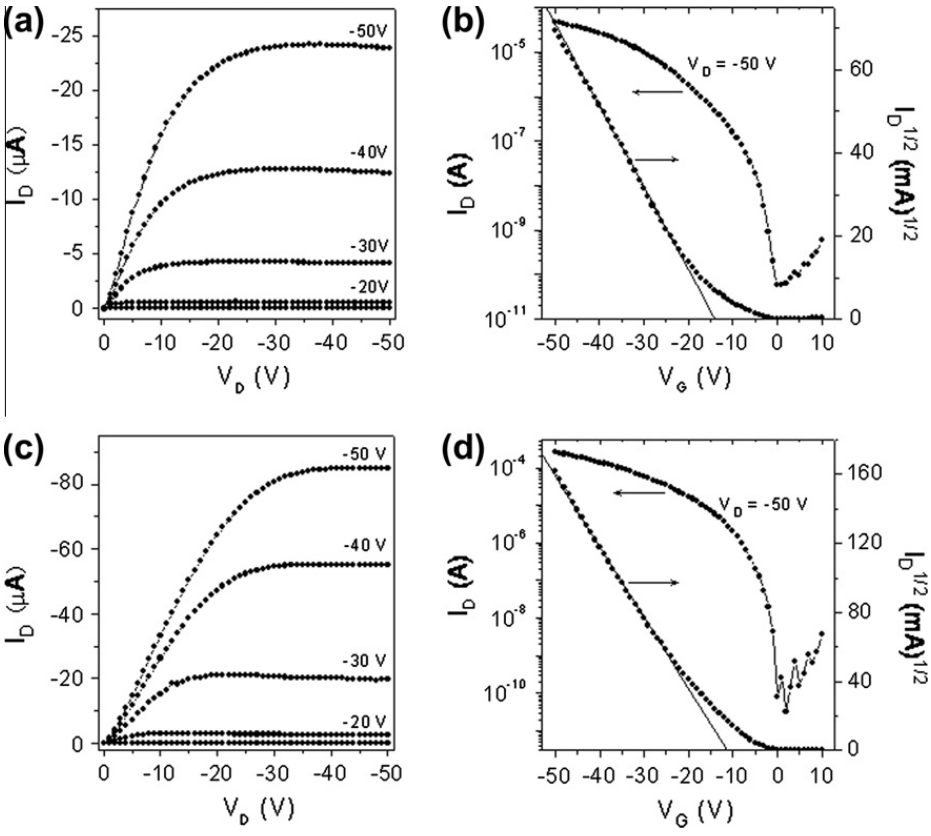

Fig. 5. Typical output (a and c) and transfer (b and d) characteristics of OTFT devices based on **Ph5T2** on ODTS (a and b) and 6P (c and d) modified Si/SiO_2 substrates at T_{sub} = 80 °C.

evaluated in ambient conditions at room temperature. The mobility was calculated from saturation region. All devices showed *p*-type transport characteristic and operated in an accumulation mode. Fig. 5 shows the typical output and transfer characteristics of OTFT devices of **Ph5T2** at the T_{sub} of 80 °C. Output curves of the devices exhibited standard linear and saturated regime and almost no noticeable contact resistance (Figs. 5a and c). On the ODTS modified substrates, **Ph5T2** exhibited mobilities up to 0.36 $cm^2 V^{-1} s^{-1}$ and a threshold voltage (V_T) of −14 V (see Fig. 5b). Device performance was not improved when HMDS and OTS were used as substrate treatment reagents. The moderate mobility of the devices of **Ph5T2** should be attributed to the coexistence of two crystalline phases as aforementioned (see Fig. 3a), which may lead to the formation of charge carrier trap sites in the semiconducting channel. From above discussion (see Figs. 3 and 4), the **Ph5T2** films on 6P modified substrates comprised only one crystalline phase, and were highly ordered both in plane and out of plane along with well-connected crystalline grains. As a consequence, the OTFT device performance of **Ph5T2** on the 6P-modified substrates was dramatically improved. Fig. 5c and d depict the typical device output and transfer characteristic, respectively. As shown in Table 1 and Fig. 5d, at the optimized T_{sub} of 80 °C, a mobility of 1.2 $cm^2 V^{-1} s^{-1}$ along with a V_T of −11 V and a I_{on}/I_{off} of 10^6 was achieved.

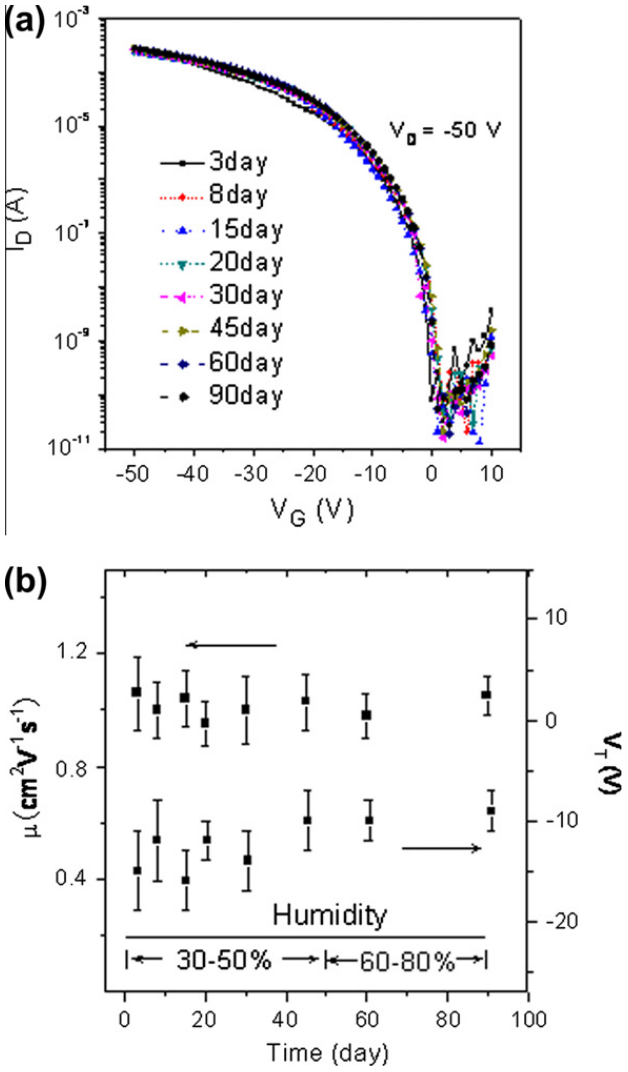

Fig. 6. (a) Transfer characteristics of OTFTs on 6P-modified substrates upon stored in ambient conditions for 3 months. (b) Average mobility and V_T of the eight devices with error bar upon stored in ambient conditions for 3 months.

The storage stability of OTFTs on 6P-modified substrates was studied in ambient condition with relative humidity varied in 30–80%. As shown in Fig. 6a, in the storage period of three months, the transfer curves remain nearly unchanged along with I_{on}/I_{off} keeping in the level of 10^6. Fig. 6b shows the average mobility and V_T from eight devices along with error as measured at different storage time. The mobility was almost constant within the range of error, and the threshold voltage shifted by less than 5 V. It is well-known that OTFTs usually exhibit lower stability at high humidity (for example: ⩾50%) [42–45]. However, the relative humidity during 45% of the time of the measurements in the current paper is >60% (see Fig. 6b). It was reported that HOMO energy level and film morphology had remarkable effects on the device stability [4,45–53]. This superior device stability of **Ph5T2** may be attributed to the combination of its low lying HOMO energy levels (−5.85 eV), tighter molecular packing and interconnection between crystalline grains (see Fig. 4b) in the film.

4. Conclusion

In conclusion, a novel easily made thienoacene-based organic semiconductor, i.e., dinaphtho[3,4-*d*:3′,4′-*d*′]benzo[1,2-*b*:4,5-*b*′]dithiophene (**Ph5T2**), was designed and synthesized. **Ph5T2** can form highly ordered films with large domain size on the 6P-modified substrates. OTFTs with mobilities up to 1.2 $cm^2 V^{-1} s^{-1}$ have been fabricated. Most importantly, the devices are highly stable and exhibit almost no performance degradation during 3 months storage under ambient conditions with relative humidity up to 80%.

Acknowledgements

This work is supported by National Basic Research Program of China (973 Project, No. 2009CB623603) of Chinese Ministry of Science and Technology, NSFC (Nos. 20921061, 50833004 and 51273192).

Appendix A. Supplementary material

Supplementary data associated with this article can be found, in the online version, at http://dx.doi.org/10.1016/j.orgel.2012.09.041.

References

[1] C.L. Wang, H.L. Dong, W.P. Hu, Y.Q. Liu, D.B. Zhu, Semiconducting π-conjugated systems in field-effect transistors: a material odyssey of organic electronics, Chem. Rev. 112 (2012) 2208–2267.
[2] K. Takimiya, S. Shinamura, I. Osaka, E. Miyazaki, Thienoacene-based organic semiconductors, Adv. Mater. 23 (2011) 4347–4370.

[3] T.W. Kelley, D.V. Muyres, P.F. Baude, T.P. Smith, T.D. Jones, High performance organic thin film transistors, Mater. Res. Soc. Symp. Proc., 771 (2003) L6.5.1-L6.5.11.

[4] H. Klauk, U. Zschieschang, R.T. Weitz, H. Meng, F. Sun, G. Nunes, D.E. Keys, C.R. Fincher, Z. Xiang, Organic transistors based on di(phenylvinyl)anthracene: performance and stability, Adv. Mater. 19 (2007) 3882–3887.

[5] R. Mondal, R.M. Adhikari, B.K. Shah, D.C. Neckers, Revisiting the stability of hexacenes, Org. Lett. 9 (2007) 2505–2508.

[6] R. Mondal, B.K. Shah, D.C. Neckers, Photogeneration of heptacene in a polymer matrix, J. Am. Chem. Soc. 128 (2006) 9612–9613.

[7] K. Xiao, Y.Q. Liu, T. Qi, W. Zhang, F. Wang, J.H. Gao, W.F. Qiu, Y.Q. Ma, G.L. Cui, S.Y. Chen, X.W. Zhan, G. Yu, J.G. Qin, W.P. Hu, D.B. Zhu, A highly π-stacked organic semiconductor for field-effect transistors based on linearly condensed pentathienoacene, J. Am. Chem. Soc. 127 (2005) 13281–13286.

[8] J.H. Gao, R.J. Li, L.Q. Li, Q. Meng, H. Jiang, H.X. Li, W.P. Hu, High-performance field-effect transistor based on dibenzo[d,d′]thieno[3,2-b;4,5-b′]dithiophene, an easily synthesized semiconductor with high ionization potential, Adv. Mater. 19 (2007) 3008–3011.

[9] Y. Miyata, E. Yoshikawa, T. Minari, K. Tsukagoshi, S. Yamaguchi, High-performance organic field-effect transistors based on dihexyl-substituted dibenzo[d,d′]thieno[3,2-b;4,5-b′]dithiophene, J. Mater. Chem. 22 (2012) 7715–7717.

[10] H. Sirringhaus, R.H. Friend, C.S. Wang, J. Leuninger, K. Müllen, Dibenzothienobisbenzothiophene – a novel fused-ring oligomer with high field-effect mobility, J. Mater. Chem. 9 (1999) 2095–2101.

[11] B. Wex, B.R. Kaafarani, R. Schroeder, L.A. Majewski, P. Burckel, M. Grell, D.C. Neckers, New organic semiconductors and their device performance as a function of thiophene orientation, J. Mater. Chem. 16 (2006) 1121–1124.

[12] P. Gao, D. Beckmann, H.N. Tsao, X. Feng, V. Enkelmann, W. Pisula, K. Müllen, Benzo[1,2-b:4,5-b′]bis[b]benzothiophene as solution processible organic semiconductor for field-effect transistors, Chem. Commun. (2008) 1548–1550.

[13] P. Gao, D. Beckmann, H.N. Tsao, X. Feng, V. Enkelmann, M. Baumgarten, W. Pisula, K. Müllen, Dithieno[2,3-d;2′,3′-d′]benzo[1,2-b;4,5-b′]dithiophene (DTBDT) as semiconductor for high-performance, solution-processed organic field-effect transistors, Adv. Mater. 21 (2009) 213–216.

[14] J.G. Laquindanum, H.E. Katz, A.J. Lovinger, Synthesis, morphology, and field-effect mobility of anthradithiophenes, J. Am. Chem. Soc. 120 (1998) 664–672.

[15] M. Chen, C. Kim, S. Chen, Y. Chiang, M. Chung, A. Facchetti, T.J. Marks, Functionalized anthradithiophenes for organic field-effect transistors, J. Mater. Chem. 18 (2008) 1029–1036.

[16] M.L. Tang, T. Okamoto, Z.N. Bao, High-performance organic semiconductors: asymmetric linear acenes containing sulphur, J. Am. Chem. Soc. 128 (2006) 16002–16003.

[17] M.L. Tang, A.D. Reichardt, T. Okamoto, N. Miyaki, Z.N. Bao, Functionalized asymmetric linear acenes for high-performance organic semiconductors, Adv. Funct. Mater. 18 (2008) 1579–1585.

[18] M.L. Tang, S.C.B. Mannsfeld, Y. Sun, H.A. Becerril, Z.N. Bao, Pentaceno[2,3-b]thiophene, a hexacene analogue for organic thin film transistors, J. Am. Chem. Soc. 131 (2009) 882–883.

[19] S. Shinamura, I. Osaka, E. Miyazaki, A. Nakao, M. Yamagishi, J. Takeya, K. Takimiya, Linear- and angular-shaped naphthodithiophenes: selective synthesis, properties, and application to organic field-effect transistors, J. Am. Chem. Soc. 133 (2011) 5024–5035.

[20] K. Takimiya, H. Ebata, K. Sakamoto, T. Izawa, T. Otsubo, Y. Kunugi, 2,7-Diphenyl[1]benzothieno[3,2-b]benzothiophene, a new organic semiconductor for air-stable organic field-effect transistors with mobilities up to 2.0 $cm^2V^{-1}s^{-1}$, J. Am. Chem. Soc. 128 (2006) 12604–12605.

[21] T. Yamamoto, K. Takimiya, Facile synthesis of highly π-extended heteroarenes, dinaphtho[2,3-b:2′,3′-f]chalcogenopheno[3,2-b]chalcogenophenes, and their application to field-effect transistors, J. Am. Chem. Soc. 129 (2007) 2224–2225.

[22] H. Ebata, T. Izawa, E. Miyazaki, K. Takimiya, M. Ikeda, H. Kuwabara, T. Yui, Highly soluble [1]benzothieno[3,2-b]benzothiophene (BTBT) derivatives for high-performance, solution-processed organic field-effect transistors, J. Am. Chem. Soc. 129 (2007) 15732–15733.

[23] T. Izawa, E. Miyazaki, K. Takimiya, Molecular ordering of high-performance soluble molecular semiconductors and re-evaluation of their field-effect transistor characteristics, Adv. Mater. 20 (2008) 3388–3392.

[24] M.J. Kang, I. Doi, H. Mori, E. Miyazaki, K. Takimiya, M. Ikeda, H. Kuwabara, Alkylated dinaphtho[2,3-b:2′,3′-f]thieno[3,2-b]thiophenes (Cn-DNTTs): organic semiconductors for high-performance thin-film transistors, Adv. Mater. 23 (2011) 1222–1225.

[25] K. Niimi, S. Shinamura, I. Osaka, E. Miyazaki, K. Takimiya, Dianthra[2,3-b:2′,3′-f]thieno[3,2-b]thiophene (DATT): synthesis, characterization, and FET characteristics of new π-extended heteroarene with eight fused aromatic rings, J. Am. Chem. Soc. 133 (2011) 8732–8739.

[26] M. Mamada, T. Minamiki, H. Katagiri, S. Tokito, Synthesis, physical properties, and field-effect mobility of isomerically pure syn-/anti-anthradithiophene derivatives, Org. Lett. 14 (2012) 4062–4065.

[27] J. Huang, H. Luo, L. Wang, Y. Guo, W. Zhang, H. Chen, M. Zhu, Y. Liu, G. Yu, Dibenzoannelated tetrathienoacene: synthesis, characterization, and applications in organic field-effect transistors, Org. Lett. 14 (2012) 3300–3303.

[28] L. Ma, P.S. White, W. Lin, Well-defined enantiopure 1,1′-binaphthyl-based oligomers: synthesis, structure, photophysical properties, and chiral sensing, J. Org. Chem. 67 (2002) 7577–7586.

[29] A. Haryono, K. Miyatake, J. Natori, E. Tsuchida, Synthesis of a novel oligo(p-phenylene) ladder by sulfide and sulfonio groups, Macromolecules 32 (1999) 3146–3149.

[30] J. Leuninger, S. Trimpin, H.-J. Räder, K. Müllen, Novel approach to ladder-type polymers: polydithiathianthrene via the intramolecular acid-induced cyclization of methylsulfinyl-substituted poly(meta-phenylene sulfide), Macromol. Chem. Phys. 202 (2001) 2832–2842.

[31] C. Wang, L.H. Jimison, L. Goris, I. McCulloch, M. Heeney, A. Ziegler, A. Salleo, Microstructural origin of high mobility in high-performance poly(thieno-thiophene) thin-film transistors, Adv. Mater. 22 (2010) 697–701.

[32] Y. Li, S.P. Singh, P. Sonar, A high mobility p-type DPP-thieno[3,2-b]thiophene copolymer for organic thin-film transistors, Adv. Mater. 22 (2010) 4862–4866.

[33] K.P. Pernstich, S. Haas, D. Oberhoff, C. Goldmann, D.J. Gundlach, B. Batlogg, A.N. Rashid, G. Schitter, Threshold voltage shift in organic field effect transistors by dipole monolayers on the gate insulator, J. Appl. Phys. 96 (2004) 6431.

[34] L.Z. Huang, F. Zhu, C.F. Liu, H.B. Wang, Y.H. Geng, D.H. Yan, Heteroepitaxy growth high performance films of perylene diimide derivatives, Org. Electron. 11 (2010) 195–201.

[35] H. Okamoto, N. Kawasaki, Y. Kaji, Y. Kubozono, A. Fujiwara, M. Yamaji, Air-assisted high-performance field-effect transistor with thin films of picene, J. Am. Chem. Soc. 130 (2008) 10470–10471.

[36] Z. Liang, Q. Tang, R. Mao, D. Liu, J. Xu, Q. Miao, The position of nitrogen in N-heteropentacenes matters, Adv. Mater. 23 (2011) 5514–5518.

[37] Y. Wang, S.D. Motta, F. Negri, R. Friedlein, Effect of oxygen on the electronic structure of highly crystalline picene films, J. Am. Chem. Soc. 133 (2011) 10054–10057.

[38] J.L. Yang, D.H. Yan, Weak epitaxy growth of organic semiconductor thin films, Chem. Soc. Rev. 38 (2009) 2634–2645.

[39] H.K. Tian, Y.F. Deng, F. Pan, L.Z. Huang, D.H. Yan, Y.H. Geng, F.S. Wang, A feasibly synthesized ladder-type conjugated molecule as the novel high mobility n-type organic semiconductor, J. Mater. Chem. 20 (2010) 7998–8004.

[40] M.J. Kang, T. Yamamoto, S. Shinamura, E. Miyazaki, K. Takimiya, Unique three-dimensional (3D) molecular array in dimethyl-DNTT crystals: a new approach to 3D organic semiconductors, Chem. Sci. 1 (2010) 179–183.

[41] T.W. Kelley, L.D. Boardman, T.D. Dunbar, D.V. Muyres, M.J. Pellerite, T.P. Smith, High-performance OTFTs using surface-modified alumina dielectrics, J. Phys. Chem. B 107 (2003) 5877–5881.

[42] I. Osaka, T. Abe, S. Shinamura, E. Miyazaki, K. Takimiya, High-mobility semiconducting naphthodithiophene copolymers, J. Am. Chem. Soc. 132 (2010) 5000–5001.

[43] I. McCulloch, M. Heeney, C. Bailey, K. Genevicius, I. Macdonald, M. Shkunov, D. Sparrowe, S. Tierney, R. Wagner, W. Zhang, M.L. Chabinyc, R.J. Kline, M.D. Mcgehee, M.F. Toney, Liquid-crystalline semiconducting polymers with high charge-carrier mobility, Nature Mater. 5 (2006) 328–333.

[44] I. Osaka, K. Takimiya, R.D. McCullough, Benzobisthiazole-based semiconducting copolymers showing excellent environmental stability in high-humidity air, Adv. Mater. 22 (2010) 4993–4997.

[45] U. Zschieschang, F. Ante, T. Yamamoto, K. Takimiya, H. Kuwabara, M. Ikeda, T. Sekitani, T. Someya, K. Kern, H. Klauk, Flexible low-voltage organic transistors and circuits based on a high-mobility organic semiconductor with good air stability, Adv. Mater. 22 (2010) 982–985.

[46] H. Meng, Z.N. Bao, A.J. Lovinger, B.C. Wang, A.M. Mujsce, High field-effect mobility oligofluorene derivatives with high environmental stability, J. Am. Chem. Soc. 123 (2001) 9214–9215.
[47] J.A. Merlo, C.R. Newman, C.P. Gerlach, T.W. Kelley, D.V. Muyres, S.E. Fritz, M.F. Toney, C.D. Frisbie, P-channel organic semiconductors based on hybrid acene–thiophene molecules for thin-film transistor applications, J. Am. Chem. Soc. 127 (2005) 3997–4009.
[48] C. Di, G. Yu, Y.Q. Liu, Y.L. Guo, X.N. Sun, J. Zheng, Y.G. Wen, Y. Wang, W.P. Hu, D.B. Zhu, Effect of dielectric layers on device stability of pentacene-based field-effect transistors, Phys. Chem. Chem. Phys. 11 (2009) 7268–7273.
[49] D. Kumaki, M. Yahiro, Y. Inoue, S. Tokito, Air stable, high performance pentacene thin-film transistor fabricated on SiO_2 gate insulator treated with β-phenethyltrichlorosilane, Appl. Phys. Lett. 90 (2007) 133511.
[50] K. Fukuda, T. Hamamoto, T. Yokota, T. Sekitani, U. Zschieschang, H. Klauk, T. Someya, Effects of the alkyl chain length in phosphonic acid self-assembled monolayer gate dielectrics on the performance and stability of low-voltage organic thin-film transistors, Appl. Phys. Lett. 95 (2009) 203301.
[51] H.E. Katz, J. Johnson, A.J. Lovinger, W. Li, Naphthalenetetracarboxylic diimide-based n-channel transistor semiconductors: structural variation and thiol-enhanced gold contacts, J. Am. Chem. Soc. 122 (2000) 7787–7792.
[52] M. Ling, P. Erk, M. Gomez, M. Koenemann, J. Locklin, Z. Bao, Air-stable n-channel organic semiconductors based on perylene diimide derivatives without strong electron withdrawing groups, Adv. Mater. 19 (2007) 1123–1127.
[53] J.H. Oh, S. Liu, Z. Bao, R. Schmidt, F. Würthner, Air-stable n-channel organic thin-film transistors with high field-effect mobility based on N,N′-bis(heptafluorobutyl)-3,4:9,10-perylene diimide, Appl. Phys. Lett. 91 (2007) 212107.